Asian Journal of Chemistry; Vol. 36, No. 6 (2024), 1403-1408

ASIAN JOURNAL OF CHEMISTRY

https://doi.org/10.14233/ajchem.2024.31664

Synthesis and Characterization of Polypyrrole-Protected Y_2O_3 Binary Composite: A Promising Electrode Material for Supercapacitors

JYOTI, KUSUM LATA and PALLAVI BHARDWAJ*

Department of Chemistry, Baba Mastnath University, Asthal Bohar, Rohtak-124021, India

*Corresponding author: E-mail: pallavibhardwaj@bmu.ac.in

Received: 6 April 2024; *Accepted*: 14 May 2024; *Published online*: 31 May 2024; AJC-21655

In this work, the synthesis and comprehensive characterization of a novel binary composite comprising polypyrrole (PPy) protected Y_2O_3 was fabricated *via in situ* oxidative-polymerization technique is presented. The investigation primarily focuses on the elucidating the structural, chemical and electrochemical properties of the synthesized composite material to assess its potential applicability as an electrode material in supercapacitors. The structural and bonding aspects of the synthesized sample were examined using advanced analytical techniques, including X-ray diffraction (XRD) and Fourier transform infrared spectroscopy (FTIR). Transmission electron microscopy (TEM) analysis was employed to confirm the synthesis of particles within the nano-range, providing the crucial insights into the morphology and size distribution of the composite. Furthermore, the chemical composition and thermal stability of the composite were evaluated through energy dispersive X-ray and thermogravimetric (TG) analyses, respectively. These analyses contributed to a comprehensive understanding of the material's composition and stability under different temperature conditions. The electrochemical performance of the PPy-Y_2O_3 nanocomposite was assessed *via* cyclic voltametric measurements, revealing a semi-rectangular loop indicative of high surface area and specific conductance. The composite displayed significant charge storage capacity and revealed exceptional ionic and electrical conductivity, highlighting its feasibility for use as an electrode material in supercapacitors. Furthermore, the synthesized PPy-Y_2O_3 nanocomposite possesses a unique combination of structural integrity, chemical stability and superior electrochemical properties, making it a promising candidate for enhancing the performance of energy storage devices, particularly in supercapacitor applications.

Keywords: Polypyrrole, Yttrium(III) oxide, Conductance studies, Electrochemical studies, Supercapacitor.

INTRODUCTION

The evolution of materials has long played a pivotal role in shaping human culture and driving the advancement of civilizations. Nanocomposites have recently emerged as a major subject of interest within the expansive field of micro and nanoscale material investigation [1,2]. Researchers have shown significant interest in this emerging discipline, focusing specifically on the synthesis, characterization, and application studies in nanoscience [3,4]. At the heart of nanoscience lies the ability to manipulate matter at the molecular level, resulting in structures with unique properties and functionalities [5]. Significant progress have been made in the development of nanomaterials, with their chemical characteristics, such as domain dimensions, molecular mixing, regularity and phase consistency, directly influencing their optical, photocatalytic, antibacterial, physical and mechanical properties [6,7].

Metal oxide nanoparticles have been extensively used in numerous fields such as phosphorescence, semiconductors, micro-electronics, biochemical and optical sensors, as well as energy storage devices like supercapacitors and rechargeable batteries [8-10]. The properties of these nanoparticles are profoundly affected by factors such as particle size, metal type and reaction parameters, highlighting the importance of precise control during synthesis [9,11].

Conducting polymers have also garnered significant attention due to their unique advantages over conventional materials, including wide electrical conductivity range, ease of manufacturing, mechanical durability and affordability [12-14]. Conducting polymers are valuable substitutes for semi-metals or replacement metals that are expensive, time-consuming and energy-intensive to extract from their source [15-17]. Polypyrrole (PPy), one of the conducting polymers, offers a number of advantages, including excellent conductivity, durability against oxid-

ation, fascinating redox properties and protection against corrosion for a variety of metallic components [18]. Commercially accessible, readily oxidized, water soluble and possessing favourable chemical characteristics, conductivity and ecological durability are pyrrole monomer units [19]. Since past two decades, PPy has attracted interest for a wide range of applications, such as pigment-sensitive solar cells, sensor technologies, memory storage, hybrid capacitors and rechargeable batteries for energy storage and more [20,21]. Polypyrrole is also employed in the production of tailored nanoparticle structures for electrochemical biosensors and storage devices, as well as for metal security purposes [22,23].

The combination of metal oxide nanoparticles and conducting polymers such as PPy can result in synergistic effects, which can boost functionality in various sectors, including energy storage, biosensors and catalytic devices [24-28]. In this context, this study aims to explore the synthesis and characterization of a novel electrode material consisting of Y_2O_3 embedded in a PPy matrix, resulting in a Y_2O_3/PPy composite. Through techniques such as X-ray diffraction (XRD), Fourier tranform infrared spectroscopy (FTIR) and transmission electron microscopy (TEM), the structure, crystallinity and particle size of the composite will be analyzed. Additionally, the electrochemical characteristics of the prepared composite will be evaluated using cyclic voltammetry and electrochemical impedance spectroscopy. This study aims to enhance our understanding of the characteristics and effectiveness of this composite material.

EXPERIMENTAL

Preparation of polypyrrole: Pyrrole monomer was polymerized using chemically oxidative process where $FeCl_3$ was used as oxidizing agent. Pyrrole (0.2 mol) was agitated in 100 mL distilled water and aqueous $FeCl_3$ (0.6 mol) was gradually added to pyrrole solution with continuous stirring (12 h) using a magnetic bar at room temperature. The obtained black precipitate was vacuum-filtered and washed thoroughly with water and ethanol. The solid PPy formed was dried in oven (50 ºC) and was transformed into an extremely fine powder [29,30].

Preparation of Y_2O_3 nanoparticles: Y_2O_3 nanoparticles were formed at a lower temperature using a combustion method. Water was utilized as a solvent, while $Y(NO_3)_3{\cdot}6H_2O$ and urea were employed as source materials. To obtain a homogeneous aqueous solution, the estimated quantity of yttrium nitrate was dissolved into a 100 mL beaker and then heated at 80 ºC. Excess water was evaporated during heating, resulting in the formation of gel-like product. A known quantity of urea was then added along with some distilled water resulting in the formation of paste before being heated. The purpose of the added urea was to dissolve the metal ions evenly in the reaction solution by forming complexes with them. For around 15 min, the paste was heated to 500 ºC in a furnace.

Preparation of PPy-Y_2O_3 nanocomposite: To prepare PPy-Y_2O_3 nanocomposite, *in situ* polymerization technique was used including a similar procedure followed for synthesis of polypyrrole. Pyrrole (0.2 mol) was agitated in 100 mL double distilled water and aqueous Y_2O_3 (0.5 g) was transferred to the former. The obtained aqueous solution was then ultra-sonically sonicated for 2 h to allow pyrrole to adsorb on surface of Y_2O_3. Then aqueous $FeCl_3$ (0.6 mol) was gradually added to obtain a suspension with continuous stirring (12 h) using a magnetic bar at room temperature. The obtain black precipitate was vacuum filtered and washed systematically water and ethanol. After that PPy-Y_2O_3 formed was dried in oven (50 ºC) and transformed into an extremely fine powder for various characterizations [30].

Characterization: The crystalline structure and phase composition of the sample were investigated by recoding the diffraction pattern of samples using Rigaku Ultima-IV diffractometer with Bragg-Brentano geometry using Cu*K*α radiation having wavelength of 1.5416 Å. X-ray pattern of the materials were recorded from 15º-70º (2θ angle) having scanning speed of 2º/min and 0.02º step interval. The IR spectral profile was recorded using an FTIR spectrometer (Perkin-Elmer 5700) using KBr as a reference. The morphology and average particle size of the samples was determined by using TECNAI (200 kV) transmission electron microscope (TEM). Elemental analysis and chemical composition of the composite was executed on Ametek (energy dispersive X-ray spectrometer). At a heating rate of 10 ºC min^{-1}, the thermograms (30-1000 ºC) of the prepared samples were recorded using a Hitachi STA 7300 thermogravimetric analyzer. The redox behaviour of the composite material was investigated using the Ivium potentiostat.

RESULTS AND DISCUSSION

X-ray diffraction studies: Using diffraction analysis, the crystal structure and phase of the prepared samples were determined. The XRD patterns of pure Y_2O_3 and PPy-Y_2O_3 nanocomposite are shown in Fig. 1. The synthesis of highly crystalline materials is indicated by the presence of strong diffraction peaks in the XRD profiles. Diffraction pattern of Y_2O_3 was found to be closely related to the cubic structure and *Ia*3 (206) space group of Y_2O_3 with JCPDS card no. 86-1326 [31,32]. Additionally, the lack of foreign peaks in the Y_2O_3 diffraction pattern demonstrated the pure synthesis of the material under consideration. Additionally, a nearly identical diffraction pattern showing a small deviation of peaks from Y_2O_3 was seen for the PPy-Y_2O_3 composite material, revealing the homogenous participation of both PPy and Y_2O_3 phases in the nanocomposite. The optimal interaction between the various phases in the nanocomposite is demonstrated by a minor change in a few peak positions [33,34].

With the help of Scherrer's formula (eqn. 1), the crystal size was calculated from FWHM of the strongest peak. The determined crystal size for Y_2O_3 and PPy-Y_2O_3 nanocomposite was found to be 34.56 and 32.98 nm, respectively.

$$D = \frac{k\lambda}{\beta\cos\theta} \quad (1)$$

k = constant, X-ray wavelength (λ) = 0.15416 nm, θ = angle of diffraction, β = full width at half maxima (FWHM), D = average crystallite size.

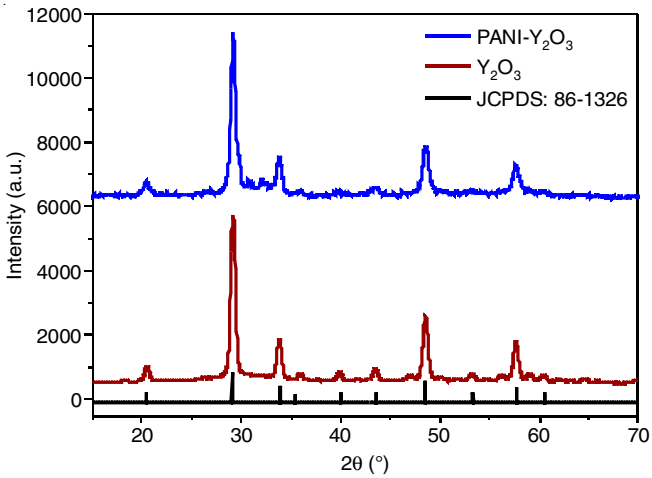

Fig. 1. Diffraction patterns of Y_2O_3 and PPy-Y_2O_3 matched with JCPDS

FTIR studies: FTIR spectrum PPy–Y_2O_3 binary composite was recorded in the range of 400-4000 cm^{-1} range to analyze its structural and bonding characteristics. The spectrum of composite material contains peaks at 919 and 814 cm^{-1} corresponding to the C–H wagging (Fig. 2). The C=C stretching vibrations are assigned to intense bands at 1607 an 1584 cm^{-1} for the oxidized states of PPy while C=N and C–N stretching appears at 1657 and 1291 cm^{-1} in the FTIR spectrum [35,36]. The presence of the quinoid and benzenoid units indicates that PPy is in the conductive emeraldine state. A broad band at 3533 cm^{-1} has been assigned to N–H stretching vibration of PPy [37]. The characteristic peaks corresponding to Y–O vibrations were observed at 703, 597 and 492 cm^{-1}.

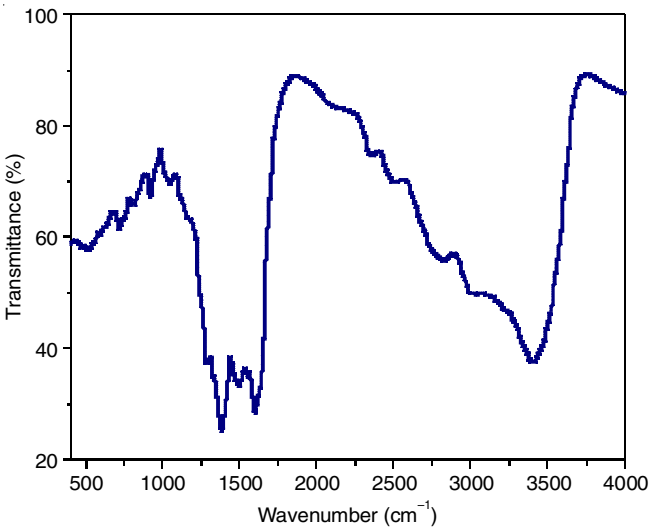

Fig. 2. FTIR spectrum of PPy-Y_2O_3 binary composite material

Morphological studies: The nearly spherical PPy-Y_2O_3 particles are observed in the TEM picture along with some aggregation (Fig. 3). The material exhibits a consistent distribution of particles with a size between 35 and 65 nm. The non-uniform dispersion of mass and heat throughout the synthetic process is responsible for the irregular shape and diverse sizes of the particles. This nanocomposite material may be useful as supercapacitor electrodes because of the production of nanoparticles.

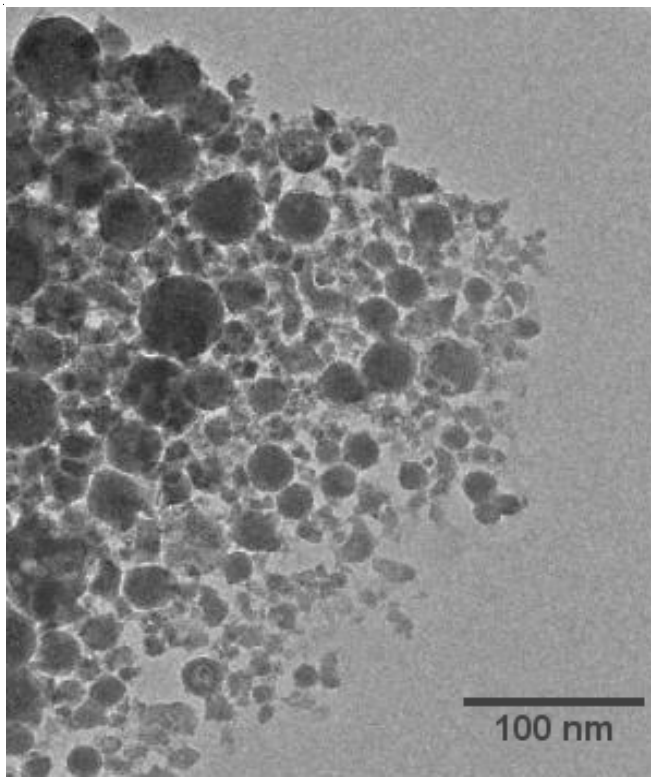

Fig. 3. TEM image of PPy-Y_2O_3 binary nanocomposite

The matching peaks for the elements included in the sample were seen when various parts of the sample were focused, as shown in Fig. 4. Only the peaks in the spectrum that match Y and O are present. The synthesis of pure PPy-Y_2O_3 nanocomposite is confirmed by the lack of peaks that correspond to the extraneous components other than the ingredients. Table-1 lists the information related to EDX spectrum of PPy-Y_2O_3 nanocomposite in terms of atomic and weight percentages. A homogeneous formation of the material with a suitable elemental dispersion encouraging structural analyses was suggested by the existence of distinctive peaks in the spectrum.

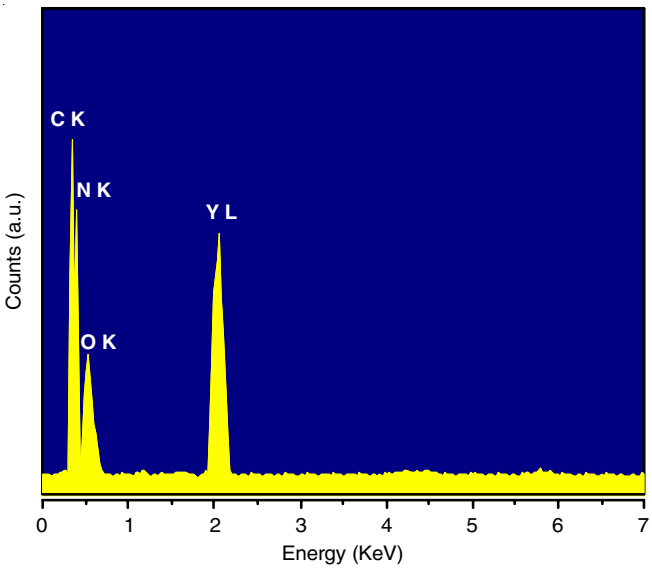

Fig. 4. EDX spectrum of PPy-Y_2O_3 nanocomposite

TABLE-1
CHEMICAL COMPOSITION OF PPy-Y_2O_3 COMPOSITE IN ATOMIC AND WEIGHT PERCENTAGE

Element	Weight (%)	Atomic (%)
C K	41.57	56.33
N K	25.79	16.98
O K	19.36	16.01
Y L	13.28	10.68

Thermal studies: To evaluate the thermal stability of the synthesized PPy-Y_2O_3 nanocomposite, the thermogravimetric analysis was carried out. The progressive weight loss transition phases, which correspond to moisture loss and the breakdown of organic matter, are revealed in temperatures range 30-900 ºC in a N_2 environment. At a lower temperature, PPy-Y_2O_3 nanocomposite starts to degrade (Fig. 5). The first weight loss of 6.54% was noted at 110 ºC which involve the elimination of H_2O molecules, weight loss of 43.89 % between 110 and 360 ºC indicated the elimination of small molecular weight oligomers and a decrease in weight of 76.23% between 360 and 680 ºC indicated the decomposition of the nanocomposite matrix. This behaviour could be the result of Y_2O_3 nanoparticles acting as catalysts, which increase the temperature at which PPy degrades. The interaction between PPy and Y_2O_3 is responsible for the PPy-Y_2O_3 nanocomposite excellent thermal stability.

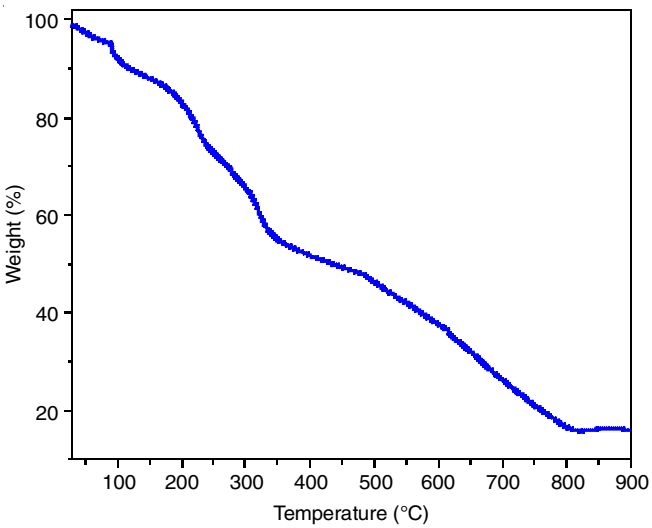

Fig. 5. Thermogravimetric curve of PPy-Y_2O_3 nanomaterial

Current-voltage measurements (I–V): The I–V characteristics of PPy-Y_2O_3 binary nanocomposite has been depicted in Fig. 6, which exhibited outstanding ohmic character at room temperature. The high conductivity of the sample approved it as excellent material for usage in electrode materials for supercapacitor.

Cyclic voltammetry (CV): In order to study the electrochemical properties of the PPy-Y_2O_3 nanocomposite, CV was carried out using a three-electrode cell construction in 1 M KOH electrolyte at a voltage (0-0.6 V). Fig. 7 exhibits the cyclic voltammogram of PPy-Y_2O_3 nanocomposite having a semi-rectangular loop of higher area indicating its higher value of specific conductance (C_{sp} = 407 Fg^{-1}) calculated as follows:

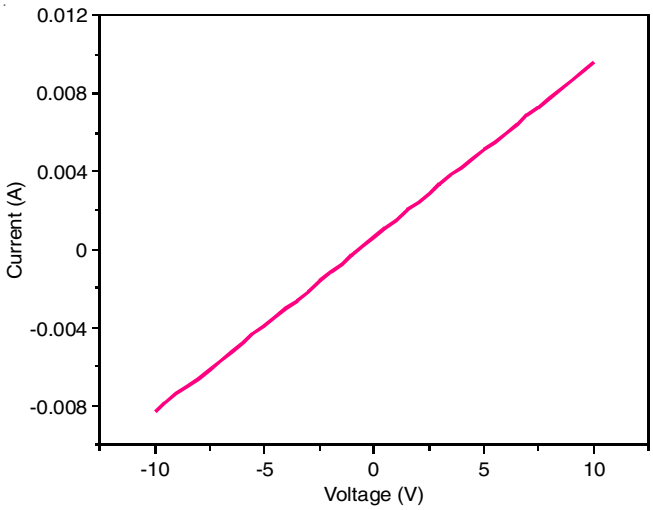

Fig. 6. I–V characteristics plot of PPy-Y_2O_3 composite

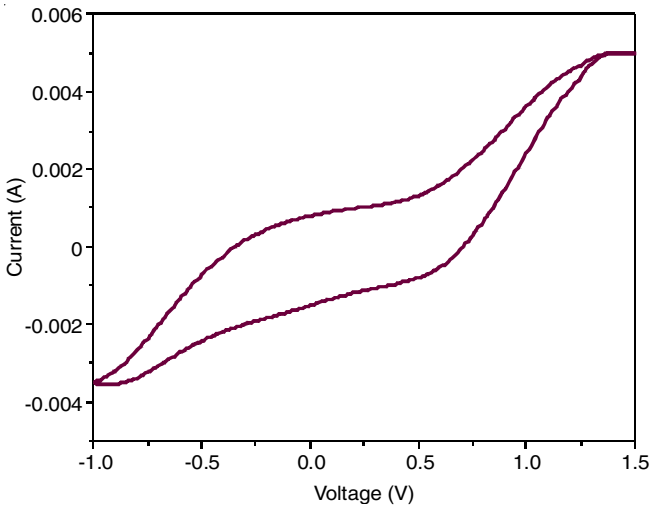

Fig. 7. Cyclic voltammogram of PPy-Y_2O_3 binary composite

$$C_{sp} = \int \frac{IdV}{smV}$$

where ∫IdV = area under the CV curve, s = sweep rate (10 mV/s), V = voltage range and m = loaded mass. The inorganic-organic association in nanocomposites, which could potentially improve the redox performance of the constructed electrode, is responsible for a high C_{sp} value.

Electrochemical impedance spectroscopic (EIS) studies: The electrochemical behaviour PPy-Y_2O_3 nanocomposite of was further explored using EIS. Nyquist plots (Fig. 8) between Z′ (real part) and Z″ (imaginary component) were used to fit the examined data of all three electrode materials in order to get net impedance (z). The linear and quasi-circular region of Nyquist plot are located in low and high-frequency zone, respectively. A compact semi-circle with small diameter indicates a high level of ionic conductivity in PPy-Y_2O_3 nanocomposite [38]. The I–V findings further supported the greater electrical conductivity. These findings indicated that the charge transfer rate is more important at the interface between the electrode and electrolyte surfaces, which therefore accounts for its high charge storage capability [39,40].

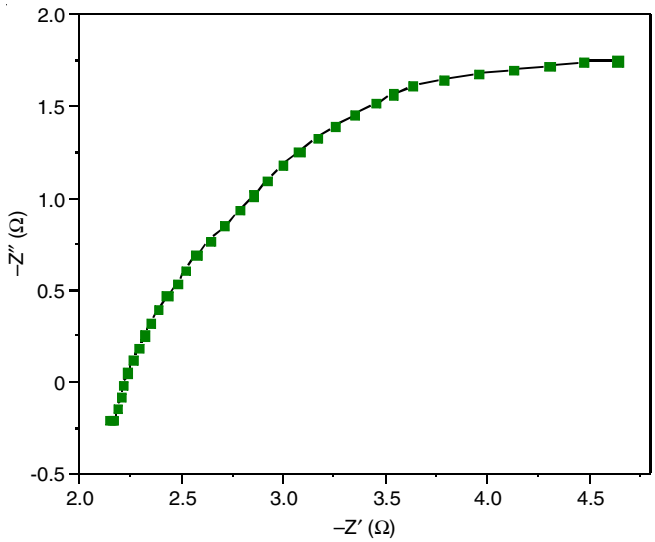

Fig. 8. Nyquist plot of PPy-Y_2O_3 binary composite

Conclusion

The Y_2O_3–PPy nanocomposite was synthesized by the *in situ* chemical oxidative method. The prepared material was characterized using XRD, FTIR, TEM, EDX, TGA, cyclic voltammetry and EIS techniques to understand the composition, structural and electrochemical properties. Diffraction data confirmed the synthesis of uncovered and PPy-covered Y_2O_3 having hexagonal crystal structure and *Ia*3 (206) space group. FTIR analysis supported XRD results exhibiting vibration bands corresponding to both PPy as well as Y_2O_3. TEM images revealed the formation of nanocomposite with some agglomeration. The TG analysis exhibited the excellent thermal stability of the sample confirming the possible interaction between PPy and Y_2O_3 in the nanocomposite. The I–V and cyclic voltammetry revealed the high ionic and electrical conductivity alongwith high charge storage capability which were further supported by Nyquist plot of PPy-Y_2O_3 nanocomposite. Due to such excellent electrochemical behaviour, PPy-Y_2O_3 nanocomposite could be used as a potential candidate for its usage as electrode material in supercapacitor.

CONFLICT OF INTEREST

The authors declare that there is no conflict of interests regarding the publication of this article.

REFERENCES

1. S. Ishaq, M. Moussa, F. Kanwal, M. Ehsan, M. Saleem, T.N. Van and D. Losic, *Sci. Rep.*, **9**, 5974 (2019); https://doi.org/10.1038/s41598-019-41939-y
2. M. Vinitha and G. Velraj, *Inorg. Nano-Metal Chem.*, (2021); https://doi.org/10.1080/24701556.2021.2018610
3. C. Ray and T. Pal, *J. Mater. Chem. A Mater. Energy Sustain.*, **5**, 9465 (2017); https://doi.org/10.1039/C7TA02116J
4. V. Van Tran, T.T.V. Nu, H.R. Jung and M. Chang, *Polymers*, **13**, 3031 (2021); https://doi.org/10.3390/polym13183031
5. P.S. Gaikar, K.S. Kadu, K.K. Tehare, G.C. Wadhawa, S.H. Mahmood and T.L. Lambat, *Nanoscale Adv.*, **4**, 5245 (2022); https://doi.org/10.1039/D2NA00654E
6. A. Varghese, K.R.S. Devi, S. Mathew, B. Saravanakumar and D. Pinheiro, *Mater. Today Proc.*, (2023); https://doi.org/10.1016/j.matpr.2023.12.003
7. A. Yadav, H. Kumar, R. Sharma, R. Kumari, G. Kumar, A. Tundwal, A. Dhayal, A. Yadav and D. Singh, *Inorg. Chem. Commun.*, **158**, 111701 (2023); https://doi.org/10.1016/j.inoche.2023.111701
8. Z.A. Hu, Y.L. Xie, Y.X. Wang, L.P. Mo, Y.Y. Yang and Z.Y. Zhang, *Mater. Chem. Phys.*, **114**, 990 (2009); https://doi.org/10.1016/j.matchemphys.2008.11.005
9. P. Singh and S.K. Shukla, *Surf. Interfaces*, **18**, 100410 (2020); https://doi.org/10.1016/j.surfin.2019.100410
10. G. Sarojini, S. Venkateshbabu and M. Rajasimman, *Chemosphere*, **278**, 130400 (2021); https://doi.org/10.1016/j.chemosphere.2021.130400
11. N. Sirotkin and A. Khlyustova, *J. Compos. Sci.*, **7**, 174 (2023); https://doi.org/10.3390/jcs7040174
12. P. Sengodu and A.D. Deshmukh, *RSC Advances*, **5**, 42109 (2015); https://doi.org/10.1039/C4RA17254J
13. N.Y. Abu-Thabit, *J. Chem. Educ.*, **93**, 1606 (2016); https://doi.org/10.1021/acs.jchemed.6b00060
14. A. Thadathil, H. Pradeep, D. Joshy, Y.A. Ismail and P. Periyat, *Mater. Adv.*, **3**, 2990 (2022); https://doi.org/10.1039/D2MA00022A
15. K. Namsheer and C.S. Rout, *RSC Adv.*, **11**, 5659 (2021); https://doi.org/10.1039/D0RA07800J
16. M. El Rhazi, S. Majid, M. Elbasri, F.E. Salih, L. Oularbi and K. Lafdi, *Int. Nano Lett.*, **8**, 79 (2018); https://doi.org/10.1007/s40089-018-0238-2
17. A.M. El-naggar, A. Alsaggaf, Z.K. Heiba, A.M. Kamal, A.M. Aldhafiri, A. Fatehmulla and M.B. Mohamed, *Opt. Mater.*, **139**, 113771 (2023); https://doi.org/10.1016/j.optmat.2023.113771
18. K. Jlassi, M.H. Sliem, F.M. Benslimane, N.O. Eltai and A.M. Abdullah, *Prog. Org. Coat.*, **149**, 105918 (2020); https://doi.org/10.1016/j.porgcoat.2020.105918
19. N. Jadhav, S. Kasisomayajula and V.J. Gelling, *Front. Mater.*, **7**, 95 (2020); https://doi.org/10.3389/fmats.2020.00095
20. M. Beygisangchin, S. Abdul Rashid, S. Shafie, A.R. Sadrolhosseini and H.N. Lim, *Polymers*, **13**, 2003 (2021); https://doi.org/10.3390/polym13122003
21. G. Shimoga, R.R. Palem, D.S. Choi, E.J. Shin, P.S. Ganesh, G.D. Saratale, R.G. Saratale, S.H. Lee and S.Y. Kim, *Metals*, **11**, 905 (2021); https://doi.org/10.3390/met11060905
22. J. Zhu, S. Wei, L. Zhang, Y. Mao, J. Ryu, P. Mavinakuli, A.B. Karki, D.P. Young and Z. Guo, *J. Phys. Chem. C*, **114**, 16335 (2010); https://doi.org/10.1021/jp1062463
23. R.K. Sharma, A.C. Rastogi and S.B. Desu, *Electrochim. Acta*, **53**, 7690 (2008); https://doi.org/10.1016/j.electacta.2008.04.028
24. F.A.G. Silva Júnior, S.A. Vieira, S.A. Botton, M.M. Costa and H.P. Oliveira, *Polímeros*, **30**, 1 (2020); https://doi.org/10.1590/0104-1428.08020
25. P. Liu, J. Yan, Z. Guang, Y. Huang, X. Li and W. Huang, *J. Power Sources*, **424**, 108 (2019); https://doi.org/10.1016/j.jpowsour.2019.03.094
26. Q.M. Al-Bataineh, A.B. Migdadi, A. Telfah, A.A. Ahmad, A.M. Alsaad and C.J. Tavares, *Mater. Chem. Phys.*, **290**, 126387 (2022); https://doi.org/10.1016/j.matchemphys.2022.126387
27. N. Abhishek, A. Verma, A. Singh, Vandana and T. Kumar, *Inorg. Chem. Commun.*, **157**, 1113334 (2021); https://doi.org/10.1016/j.inoche.2023.111334
28. A. Yadav, H. Kumar, R. Kumari and R. Sharma, *Mater. Sci. Eng. B*, **286**, 116085 (2022); https://doi.org/10.1016/j.mseb.2022.116085
29. A. Batool, F. Kanwal, M. Imran, T. Jamil and S.A. Siddiqi, *Synth. Met.*, **161**, 2753 (2012); https://doi.org/10.1016/j.synthmet.2011.10.016
30. M.U. Shariq, A. Husain, M. Khan and A. Ahmad, *Polym. Polymer Compos.*, **29(9_suppl)**, S989 (2021); https://doi.org/10.1177/09673911211036589

31. Z. Wei-Wei, Y. Min, H. Xing-Dao and G. Yi-Qing, *J. Alloys Compd.*, **509**, 3613 (2011); https://doi.org/10.1016/j.jallcom.2010.12.110
32. X.T. Wei, J.B. Zhao, Y.H. Chen, Y. Min and L. Yong, *Chin. Phys. B*, **19**, 077804 (2010); https://doi.org/10.1088/1674-1056/19/7/077804
33. R. Nekooie, T. Shamspur and A. Mostafavi, *J. Photochem. Photobiol. Chem.*, **407**, 113038 (2021); https://doi.org/10.1016/j.jphotochem.2020.113038
34. K.B. Yazhini, X. Wang, Q. Zhou and B.O. Stevy, *RSC Adv.*, **11**, 36379 (2021); https://doi.org/10.1039/D1RA07460A
35. V.Q. Trung, D.N. Tung and D.N. Huyen, *J. Exp. Nanosci.*, **4**, 213 (2009); https://doi.org/10.1080/17458080903115361
36. M. Joulazadeh and A.H. Navarchian, *Synth. Met.*, **210**, 404 (2015); https://doi.org/10.1016/j.synthmet.2015.10.026
37. M.A. Chougule, S.G. Pawar, P.R. Godse, R.N. Mulik, S. Sen and V.B. Patil, *Soft Nanosci. Lett.*, **1**, 6 (2011); https://doi.org/10.4236/snl.2011.11002
38. H. Deng, J. Huang, Z. Hu, X. Chen, D. Huang and T. Jin, *ACS Omega*, **6**, 9426 (2021); https://doi.org/10.1021/acsomega.0c05953
39. M.N. ur Rehman, T. Munawar, M.S. Nadeem, F. Mukhtar, U.A. Akbar, S. Manzoor, A.S. Hakeem, M.N. Ashiq and F. Iqbal, *Solid State Sci.*, **128**, 106883 (2022); https://doi.org/10.1016/j.solidstatesciences.2022.106883
40. M.T. Ansar, A. Ali, G.M. Mustafa, F. Afzal, S. Ishaq, F. Kanwal, S. Naseem and S. Atiq, *J. Alloys Compd.*, **855**, 157341 (2021); https://doi.org/10.1016/j.jallcom.2020.157341